Head Group and Chain Behavior in Biological Membranes: A Molecular Dynamics Computer Simulation

Alan J. Robinson,* W. Graham Richards,* Pamela J. Thomas,‡ and Michael M. Hann§
Physical Chemistry Laboratory,* Oxford University; Glaxo Research and Development,‡ Ware, Herts; and Glaxo Research and Development,§ Greenford, Middlesex, United Kingdom

ABSTRACT A computer-modeled hydrated bilayer model of the lipid 2,3-dimyristoyl-D-glycero-1-phosphorylcholine in the L_α phase was built. Particular care was taken in building the starting structure with the inclusion of structural detail reported in experiments on the L_α phase. Molecular dynamics simulations using the molecular dynamics and energy refinement program AMBER 3.1 force field with an optimized parameters for liquid simulation parameter set were run to study the motions and conformations of the lipid molecules and characterize the behavior and structure of the head groups and the hydrocarbon lipid chains. Although the head groups were observed to show great flexibility, certain head-group torsion combinations appeared favored. The observed tilt of the lipid chains is discussed and is consistent with previous experimental findings. Motion of the lipid chains is shown to be correlated with those chains immediately surrounding, but correlation with chains more distant varies with time.

INTRODUCTION

Membranes form the barrier between the cell cytoplasm and its surroundings, a barrier that many drugs and molecules must cross. The conventional model of a biological membrane is a lipid bilayer in which are embedded many proteins and sterols (Cevc and Marsh, 1987) all held together by noncovalent interactions. Interest in modeling bilayer membranes using molecular dynamics has increased dramatically (Bassolino-Klimas et al., 1993; Biswas and Shurmann, 1991; Charifson et al., 1990; Damodaran et al., 1992; Damodaran and Merz, 1993, 1994; Edholm et al., 1983; Edholm and Johansson, 1987; Edholm and Nyberg, 1992; Egberts and Berendsen, 1988; Essex, 1992; Fukada et al., 1993; Heller et al., 1993; Khalatur and Pavlov, 1987; Marrink et al., 1993; van der Ploeg and Berendsen, 1982, 1983; Stouch et al., 1991, 1994; Stouch, 1993; Venable et al., 1993; Xiang, 1993). Of these only a few have been attempts with phospholipid molecules and explicit solvent (Damodaran et al., 1992; Damodaran and Merz, 1993, 1994; Essex, 1992; Heller et al., 1993; Stouch, 1993; and Venable et al., 1993). The aim of this work is to understand biological membranes by using computer modeling to provide structural information that is difficult to obtain from conventional experiments and thence study the interactions between drugs, membranes, membrane-bound water, and other molecules.

Thus far molecular dynamics simulations have focused predominantly on the behavior of the lipid hydrocarbon chains (see references cited above) and on the waters surrounding the lipid head groups (Alper et al., 1993a, b; Berkowitz and Raghavan, 1991; Damodaran and Merz, 1993; Marrink et al., 1993; Nicklas et al., 1991). The structure of the head groups has not yet been fully characterized, but they will have large interactions with other molecules because of their charged groups. It is possible that lipids cause conformational changes in membrane proteins necessary for their function and that the interaction of drugs with hydrated head groups is a key step in passive diffusion through the membrane. Thus there is an important need to understand the behavior and structure of the head group layer.

MATERIALS AND METHODS

2,3-dimyristoyl-D-glycero-1-phosphorylcholine (DMPC; Fig. 1) was studied and exists in a number of phases. The x-ray structure of enantiomerically pure DMPC in the L_β phase has been solved (Pearson and Pascher, 1979). The unit cell has the DMPC molecule in two different conformations with the phosphatidylcholine groups being approximate mirror images. The lipids are packed as a bilayer with one of the lipid conformations displaced so that the head groups of a layer do not all lie in the same plane. The hydrocarbon chains are close packed, have an all-*trans* conformation, and make an angle of 12° with the bilayer normal.

DMPC has a head group-packing cross section that is larger than the cross section of the two hydrocarbon chains, and this is the source of the relative displacement of lipids in DMPC compared with lipids with smaller head-group cross sections, which have all the head groups coplanar, e.g., 1,2-dilauroyl-glycero-3-phosphoethanolamine (Pascher et al., 1992). For the hydrocarbon chains to be close packed in the L_β phase requires the head groups to adopt conformations and packing, which reduces their packing cross section. Furthermore, the L_β and L_α phases of DMPC differ in the surface area per lipid, 47 Å^2 in the L_β phase but at least 60 Å^2 in the L_α phase (Nagle, 1993, and references therein); hence, the lipid molecules within the crystalline L_β structure experience very different forces from those present in the fluid L_α phase. A model with the lipid molecule conformations based on those of the DMPC L_β crystal structure is not ideal for simulations of the L_α phase. For any model of a lipid bilayer, there are two main structural considerations, the conformations of the lipid molecules and how they pack together.

In their DMPC model, Damodaran and Merz (1993) constructed the bilayer from the crystal structure by simply increasing the separation of the constituent lipid molecules such that the head group surface area of a lipid was ~68 Å^2. Essex (1992) used a similar method but also reduced the extent

Received for publication 23 December 1993 and in final form 6 September 1994.

Address reprint requests to Dr. W. Graham Richards, Physical Chemistry Laboratory, Oxford University, South Parks Road, Oxford OX1 3QZ UK. Tel.: 44-864-275406; Fax: 44-865-275410. E-mail: gr@vax.ox.ac.uk

0006-3495/94/12/2345/10 $2.00

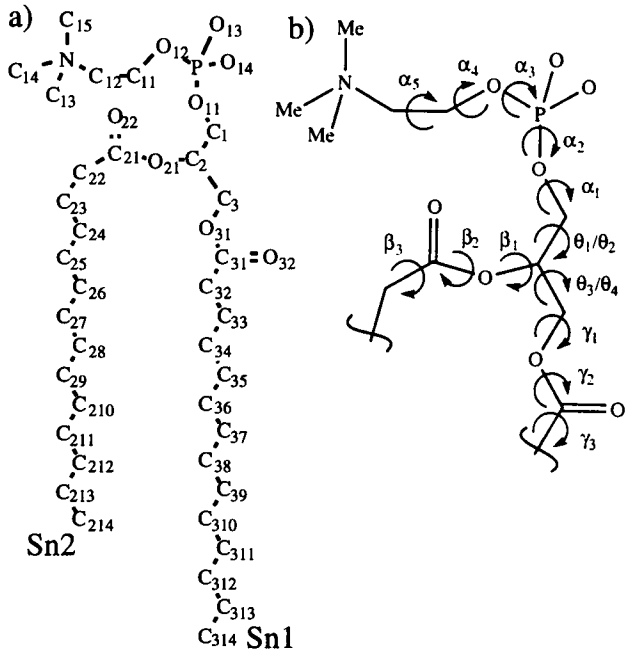

FIGURE 1 Schematic structure of DMPC illustrating (*a*) the atom numbering scheme and (*b*) the head-group torsional angles as defined by Sundaralingham (1972).

of staggering between the two crystal structure conformations. Heller et al. (1993) built their monolayer from 25 units consisting of four 1-palmitoyl-2-oleoyl-*sn*-glycero-3-phosphatidylcholine (POPC) molecules arranged by hand. The POPC molecule was built within QUANTA (MSI, 1992) and, except at the unsaturated bond, had all dihedrals (including those of the head group) as *trans*. The system was gradually equilibrated using a combination of molecular dynamics and energy refinement. Venable et al. (1993) used the elegant method of producing 72 different lipid conformations from a Monte Carlo simulation with a Marcelja field and placing these onto a two-dimensional hexagonal lattice to avoid long equilibration times. The relative orientations of the lipid molecules are not described. Stouch (1993) describes his starting structure as two monolayers of 18 DMPC molecules in a periodic box with lateral dimensions of 34.5 × 34.5 Å giving a head-group surface area of 66 Å^2/lipid.

Information from experiments investigating the structure of lipids in the fluid phase as well as the lipid crystal structure was used in building the starting structure presented here. (Seelig et al., 1977; Seelig, 1978; Lewis and Engelman, 1983; Hauser et al., 1981; Pascher et al., 1992; Pearson and Pascher, 1979; Nagle, 1993; Skarjune and Oldfield, 1979; Hauser et al., 1988; Mayer et al., 1988; Pascher and Sundell, 1986; Büldt et al., 1978, 1979; Seelig and Seelig, 1974).

The lipid molecule is divided into three components, the head group, the glycerol moiety, and the hydrocarbon chains. Structural information on these components in the L_α phase is available from ^{2}H and ^{31}P NMR and x-ray and neutron diffraction experiments (Seelig et al., 1977; Seelig, 1978; Lewis and Engelman, 1983; Hauser et al., 1981; Pascher et al., 1992; Pearson and Pascher, 1979; Nagle, 1993; Skarjune and Oldfield, 1979; Hauser et al., 1988; Mayer et al., 1988; Büldt et al., 1978, 1979; Seelig and Seelig, 1974).

The DMPC head-group conformation is described by the five α_i dihedrals shown in Fig. 1 *b*. ^{2}H and ^{31}P NMR experiments on the L_α phase (Seelig et al., 1977; Seelig, 1978; Skarjune and Oldfield, 1979) are not consistent with a model in which the polar head groups exhibit a completely flexible or completely rigid head group structure. Seelig et al. (1977) and Seelig (1978) propose two enantiomeric conformations (t, g^+, g^+, t, g^-) and (t, g^-, g^-, t, g^+) for the dihedrals (α_1, α_2, α_3, α_4, α_5), which are in rapid dynamic equilibrium. Skarjune and Oldfield (1979) conclude that the head groups adopt a limited range of conformations by searching a restricted conformational space of ±40° in 2° increments from the crystal structure dihedral angles. These conclusions are also consistent with the range of energetically most stable conformations of glycero-phosphatidylethanolamine calculated by Frischleder et al. (1981). The two conformations for (α_1, α_2, α_3, α_4, α_5) reported by Seelig et al. (1977) were used in the starting structure.

In the L_β crystal structure the dihedral θ_3 is *trans*. However, ^{1}H spin-coupling measurements on the L_α fluid phase by Hauser et al. (1988) indicate that three rotamers with θ_3 as *trans*, *gauche*$^+$ and *gauche*$^-$ exist in equilibrium. These are denoted *A*, *B*, and *C*, respectively, and occur in the ratio 6.5:5:1. Furthermore, relaxation studies by Mayer et al. (1988) indicate rotational jumps between two conformers about the glycerol C_2—C_3 bond. Molecular dynamics simulations starting with only the *trans* dihedral about the C_2—C_3 bond produced <15% of the *gauche*$^+$ rotamer and none of the *gauche*$^-$in simulations of >400 ps (Essex, 1992; A. J. Robinson, unpublished results). For more realistic simulations the alternative *B* rotamer was included in the starting structure. The source of the coordinates for this alternative glycerol rotamer was $DLPEME_2$, which crystallizes with the *gauche*$^+$ conformation at θ_3 (Pascher and Sundell, 1986) and differs from PC by possessing one less methyl on the *N*-methyl of the head group. The starting structure of the bilayer model had half the lipids with coordinates for the glycerol and the esters taken from the DMPC crystal structure. The other half had the coordinates from the $DLPEME_2$ crystal structure, which necessitated adjusting the dihedral θ_1 so the P—N dipole was nearly perpendicular to the bilayer normal as reported in ^{31}P NMR (Yeagle, 1977) and neutron diffraction studies (Büldt et al., 1978, 1979).

Finally, coordinates for the hydrocarbon chains were taken from the L_β crystal structure of DMPC; the dihedral angles of the two starting lipid conformations are listed in Table 1.

Since molecular dynamics was done in the NVT ensemble it is essential to have the dimensions of the model identical to those of a system under normal atmospheric conditions; i.e., the value of the surface area per lipid must be accurately known. Many values for this have been published (see Nagle, 1993, and references therein), and a value of 66 Å^2 was used.

Thus, 20 lipids were regularly arranged on a hexagonal lattice to form a monolayer with the relative orientation of the P-N dipoles of the head groups similar to that observed in the L_β crystal structure of DMPC (see Fig. 2) and leads to the hydrocarbon chains being arranged on an approximate square lattice. Two monolayers were put together to form a bilayer with a 35-Å P-P separation across the bilayer. This is within the value of 34 ± 1 Å measured from x-ray scattering (Lewis and Engelman, 1983) and ^{2}H NMR (Seelig and Seelig, 1974) and meant the chains of the two layers were interdigitated at the bilayer center in the starting structure (see Fig. 3). 942 TIP3P water molecules (Jorgensen et al., 1983) were added and penetrated down to the carbonyl groups of the lipid ester linkages. The presence of water here has been verified by Raman spectroscopy (Blechner et al., 1990).

The molecular dynamics and energy refinement program AMBER 3.1 (Singh et al., 1988) was used for the simulation of the membrane. The lipid was constructed as a three-residue molecule: the head group as the first residue, the glycerol and Sn1 chain as the second and the Sn2 chain as the third. The bond-stretching, angle-bending, and dihedral energy terms are contained in the standard AMBER force field except the parameters for the ester groups, which are those obtained by Charifson et al. (1990). The non-bonded parameters and partial charges were based on the OPLS united atom

TABLE 1 The dihedral angles of the two geometries in the MD starting structure

Lipid	α_1	α_2	α_3	α_4	α_5	θ_1	θ_2	θ_3	θ_4	β_1	β_2	β_3	β_4	γ_1	γ_2	γ_3	γ_4
DMPC1	−170°	60°	64°	145°	−81°	58°	177°	54°	−60°	148°	173°	−57°	176°	129°	−167°	166°	175°
DMPC2	170°	−60°	−64°	−145°	81°	168°	−82°	166°	51°	120°	179°	−134	67°	102°	176°	180°	180°

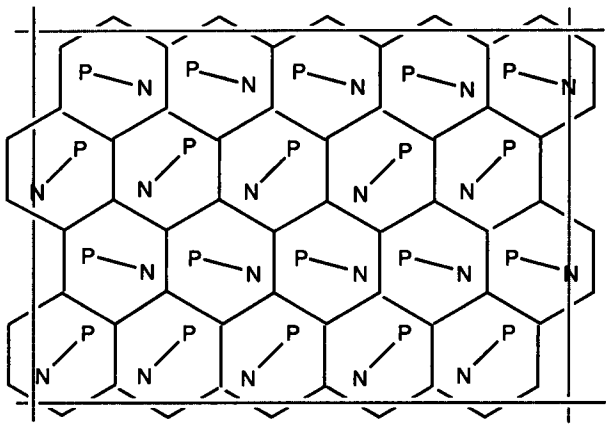

FIGURE 2 Schematic diagram of the surface of the membrane starting structure illustrating the hexagonal packing of the head groups and the relative orientation of the P-N dipoles. The dashed lines indicate the edges of the periodic box.

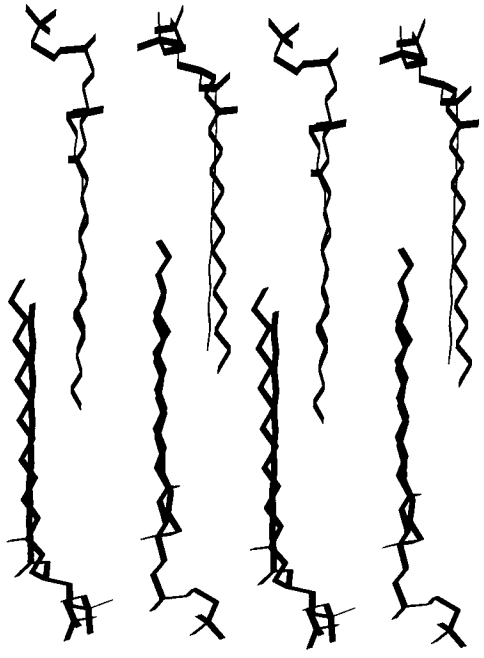

FIGURE 3 Side view of the starting structure of the DMPC bilayer, excluding waters, illustrating the interdigitation of the chains at the bilayer center and the flat surface of the membrane.

parameter set of Jorgensen et al. (1983), as previously used by Essex (1992) and are completely consistent with TIP3P waters.

A residue-based cutoff of 9 Å was applied for nonbonded interactions and the nonbonded pair list was updated every 50 fs. When calculating the dihedral energy, the van der Waals energy was reduced by a factor of eight and the electrostatic energy by a factor of two as recommended when using AMBER united atom and OPLS parameter sets with AMBER 3.1 (Jorgensen and Tirado-Reeves, 1988). Improper torsions were defined to stop the chiral center of DMPC from racemizing (C_2 in Fig. 1 *a*) and to ensure the planarity of the ester groups. The system temperature was maintained at 323 K using the Berendsen algorithm (Berendsen et al., 1984) with a relaxation time of 100 fs. The time step was 5 fs with the bond lengths constrained using the SHAKE algorithm (Ryckaert et al., 1977).

The waters and then the lipids of the starting structure were energy refined. With the head groups and waters constrained, 200 ps of molecular dynamics (MD) on the hydrocarbon chains were run. This disordered the hydrocarbon chains by introducing *gauche* dihedrals, which characterize the fluid phase, and reduced the extent of interdigitation of the chains at the interface of the two layers.

Before full MD calculations, an energy refinement of all atoms was done followed by 10 ps of MD on the waters to equilibrate the structure around the head groups. All atoms were energy refined followed by a short MD simulation with a time step of 2 fs. 200 ps of MD with a time step of 5 fs were run and treated as an equilibration phase. A subsequent 200 ps of MD were run and analyzed using a program written by Essex (1992). Two vectors were used to describe each lipid chain. The first connects C_{31} to C_{37} of Sn1, and C_{21} to C_{27} of Sn2. The second connects C_{37} to C_{314} of Sn1, and C_{27} to C_{214} of Sn2. These were called, respectively, the vectors for the upper and lower parts of the hydrocarbon chain.

RESULTS AND DISCUSSION

Fig. 4 shows the lipid bilayer after 200 ps of simulation on the lipid chains; the lipid chains are melted, the free volume between lipids has been filled, and the interdigitation of the chains at the bilayer center has disappeared. Fig. 5 shows the lipid bilayer after 400 ps of simulation on all atoms with the head groups shown in bold. During the course of the simulation head groups are observed to move in and out of the plane formed by surrounding head groups.

Previous simulations of phospholipid bilayers have not fully characterized the conformational behavior of the head groups but discussed the orientation of the P-N vector with the bilayer surface (e.g., Heller et al., 1989; Damodaran et al., 1992). Stouch (1993) notes that the head groups exhibit a number of conformations and that motion about some tor-

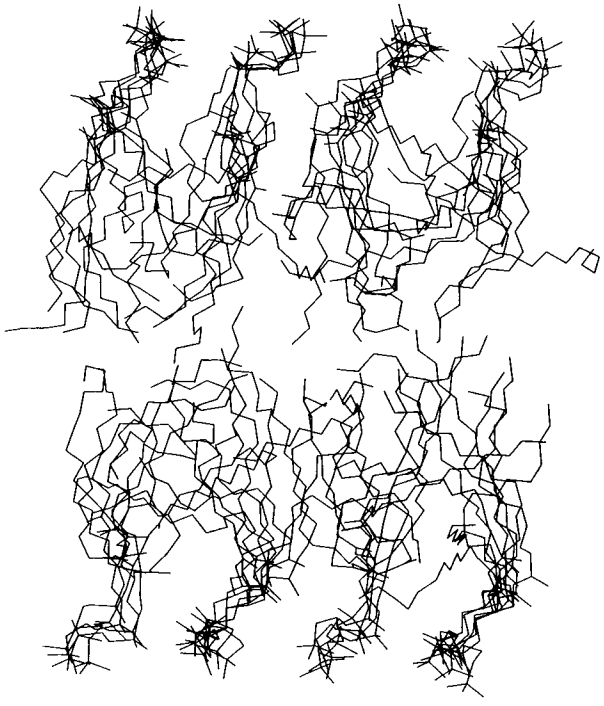

FIGURE 4 The bilayer structure after 200 ps molecular dynamics on the hydrocarbon chains only. Compared with Fig. 3 the chains are no longer interdigitated at the bilayer center, and the free volume between the chains has decreased.

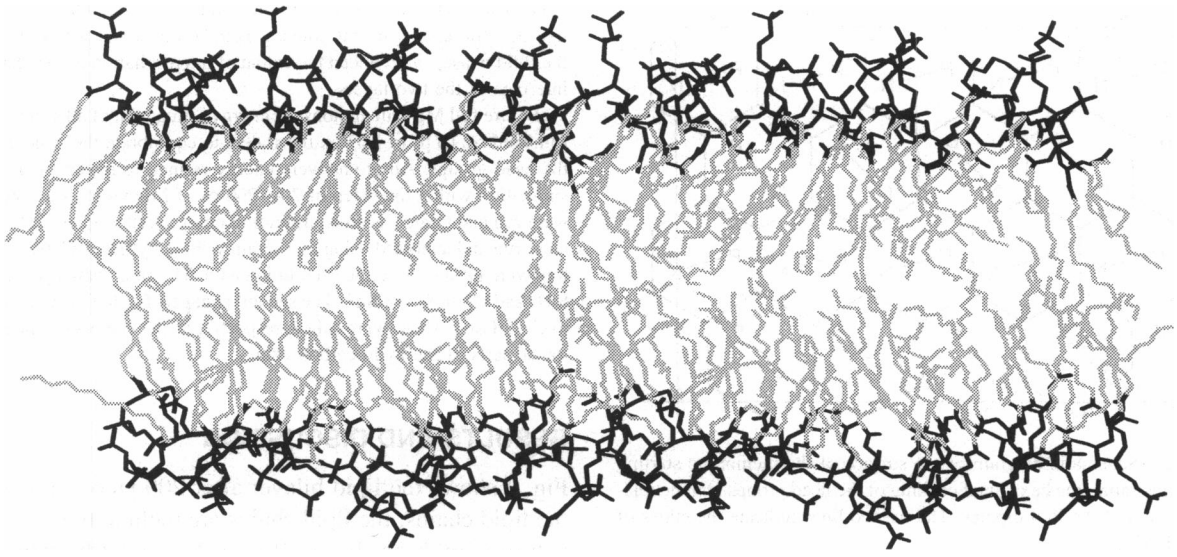

FIGURE 5 Two neighboring periodic boxes from the final dynamics frame of the simulation after 400 ps on all atoms. Waters are not shown, the head groups are colored black, and the rest of the lipid is colored gray.

sions is limited. Essex (1992) gives a description of conformations observed.

Considerable effort has gone into attempting to deduce the conformation of head groups in biological membranes, but the picture is still not clear. Techniques include ^{31}P, ^{14}N, ^{1}H, and ^{2}H NMR; neutron diffraction; and infrared spectroscopy (see Büldt and Wohlgemuth, 1981). Because of the fluid nature of the L_α phase, the NMR data are often difficult to interpret and involve comparing calculated deuterium quadripole splittings and phosphorus chemical-shift anisotropies for models of head-group structure with experimental values to evaluate possible torsional angles. The two limiting scenarios are completely free rotation in the head groups, which was dismissed by Seelig et al. (1977), and a completely rigid head group structure, which was shown to be consistent with experimental deuterium quadripole splittings and phosphorus chemical-shift anisotropies but not with the T_1 deuterium relaxation times for head-group hydrogens (Büldt and Wohlgemuth, 1981). Akutsu and Nagamori (1991) deduced the conformation of the polar head group of phosphatidylcholine in a liquid crystal bilayer to be close to one of those observed in the DMPC crystal structure. The belief now from experimental data is that the two conformations observed in crystal structures are the most probable in the liquid crystalline state and interconvert via other conformations (Skarjune and Oldfield, 1980; Seelig et al., 1977; Gally et al., 1975). Dufourc et al. (1992) deduced from pulsed ^{31}P-NMR of DMPC that the θ_1 and α_1 torsions both showed hindered rotation but that α_2 torsion exhibited free rotation. However, using Raman spectroscopy Bicknell-Brown et al. (1982) studied head-group geometry and motional freedom in aqueous dispersions of dipalmitoylphosphatidylcholine (DPPC). They concluded that there must be considerable motional freedom about the C—O bonds in the phospholipid head group, i.e., α_1 and α_4, and that this was greater than that of the P—O bonds, i.e., α_2 and α_3. Gally et al. (1975) proposed the choline moeity to have a flexible temperature-dependent conformation and described the choline group as having a bent structure, which placed the ammonium and phosphate groups in close proximity, the stability of which increased with temperature. This result is consistent with Raman spectroscopy by Akutsu (1981) on the stretching vibration of C—N bonds, which showed that α_5 should be predominantly *gauche*.

The starting structure has only two head-group conformations but during MD other conformations appear rapidly, and within 70 ps of the equilibration simulation there is already a large range present. Table 2 lists the fractional populations of the dihedrals α_1–α_5, and Table 3 lists the fractions of the head-group structures described by α_2, α_3, and α_4. Generally α_5 is almost exclusively *trans*, and α_1 is predominantly *trans*. α_2 and α_3 both show a high fraction of *gauche* dihedrals, and α_4 has a >50% probability of being *trans*. Interestingly, with the exception of α_5, the most probable dihedral angles are the same as those in the crystal structure as speculated from experiments. Furthermore, the most probable dihedral sequence of (α_2, α_3, α_4) is ($g^{\pm}$, $g^{\pm}$, t), which 26% of the head groups exhibit. This is the same sequence as in the initial starting structure and the crystal structure. Since during the 200-ps equilibration run the percentage of the (g^+, g^+, t) conformers fell as low as 5% this is unlikely

TABLE 2 The fractional populations of each of the α_i head-group dihedrals for the 200-ps MD simulation (the fraction of *gauche* bonds is further divided into the fraction of *gauche*$^+$ and *gauche*$^-$)

Dihedral	*trans*	*gauche*	*gauche*$^+$	*gauche*$^-$
α_1	67%	33%	8%	25%
α_2	27%	73%	36%	37%
α_3	26%	74%	36%	37%
α_4	56%	44%	18%	26%
α_5	82%	18%	6%	12%

TABLE 3 The fractional populations of the 27 head-group structures defined by (α_2, α_3, α_4) and the nine by (α_2, α_3) from 200 ps of MD

(α_2, α_3, α_4)	Fractional population	(α_2, α_3, α_4)	Fractional population	(α_2, α_3)	Fractional population
(g^+, g^+, t)	13.0%	(g^-, g^-, t)	13.3%	(g^+, g^+)	21.7%
(g^+, g^+, g^+)	4.1%	(g^-, g^-, g^-)	4.8%	(g^-, g^-)	21.3%
(g^+, g^+, g^-)	4.6%	(g^-, g^-, g^+)	3.2%	(t, g^+)	10.5%
(g^+, t, t)	4.0%	(g^-, t, t)	4.8%	(t, g^-)	10.8%
(g^+, t, g^+)	4.1%	(g^-, t, g^-)	4.8%	(g^+, t)	10.0%
(g^+, t, g^-)	1.9%	(g^-, t, g^+)	2.0%	(g^-, t)	11.6%
(t, g^+, t)	8.1%	(t, g^-, t)	4.1%	(g^-, g^+)	4.8%
(t, g^+, g^+)	0.35	(t, g^-, g^-)	3.9%	(g^+, g^-)	4.7%
(t, g^+, g^-)	2.1%	(t, g^-, g^+)	2.8%	(t, t)	4.8%
(t, t, g^+)	0.9%	(t, t, g^-)	2.6%		
(t, t, t)	1.3%				
(g^+, g^-, t)	3.3%	(g^-, g^+, t)	4.4%		
(g^+, g^-, g^-)	1.1%	(g^-, g^+, g^+)	0.1%		
(g^+, g^-, g^+)	0.3%	(g^-, g^+, g^-)	0.3%		

to be due to poor equilibration. The simulation behavior of α_5 is inconsistent with experimental results (Akutsu, 1981). This may be a problem with the simulation method or parameters that cannot model accurately the close electrostatic interactions between the negative phosphate and positive nitrogen moiety of a lipid molecule using partial charges. It would be expected that α_5 should be *gauche* to allow these groups to minimize their separation.

For the dihedral sequence (α_2, α_3) responsible for the bend in the head group it is evident there is not an even distribution of structures. 43% possess the ($g^{\pm}$, $g^{\pm}$) pattern, another 43% all have at least one *gauche* dihedral, <10% have two *gauche* dihedrals of opposite sign, and only 4.8% have both dihedrals being *trans*. Thus there is a much greater range of head-group conformations than proposed by Skarjune and Oldfield (1979), but the head groups are not totally flexible and interactions between neighboring lipids may be responsible for this with a preference for *gauche* dihedrals to minimize the distance between opposite charged groups in the zwitterionic head group.

Analysis of the dynamics shows the average dipole moment of the head groups to lie at an angle of 5° to the bilayer surface, i.e., the phosphorus and nitrogen lie in almost the same plane. Furthermore the carbon atoms, C_{11}, C_{12}, and those of the *N*-methyl of the choline head group from the bilayer center are approximately equidistant from the bilayer center. (Actual values are respectively 17.9 Å, 18.2, and 18.5 Å $\mp$ ~3 Å SD). This is consistent with the neutron diffraction data of Büldt et al. (1978, 1979), the conclusions of Lesslauer et al. (1972) from x-ray diffraction experiments on DMPC, the data from neutron diffraction of selectively deuterated lipids by Seelig et al. (1977), and the ζ potential data of Makino et al. (1991), which showed the orientation of the head groups to be dependent on temperature and ionic strength.

Table 4 lists the fractional populations of the three conformations of the glycerol θ_3 dihedral. In agreement with the conclusions of Hauser et al. (1988) the glycerol region is observed not to be rigid with conformation *A* being the more probable. Other simulations (data not shown) have also shown a small proportion (<4%) of the *C* rotamer occurring.

The fluidity of the hydrocarbon chains arises from the rotations about the C—C bonds of the hydrocarbon chains.

TABLE 4 The fractional populations of the three rotamers of the θ_3/θ_4 dihedral

Rotamer (θ_3, θ_4)	Population from NMR on DPPC*	Population from 200 ps MD
A (t, g^+)	52.0%	56.8%
B (g^+, g^-)	40.0%	43.2%
C (g^-, t)	7.5%	0.0%

* Edholm et al. (1983)

However, bond rotation in a chain is not completely free because of the presence of neighboring hydrocarbon chains. A single *gauche* dihedral in the upper part (i.e., near the glycerol moiety) of the hydrocarbon chain will produce a large tilt in the hydrocarbon chain with respect to the bilayer normal leading to collisions with neighboring chains and an unfavorable disruption of hydrocarbon chain packing. However, a (g^+, t, g^-) or (g^-, t, g^+) sequence of three dihedral angles, called a kink, does not cause a large change in its direction. The rotational isomeric model (Cevc and Marsh, 1987; Seelig and Seelig, 1974) proposes that *gauche* conformations in the upper part of the hydrocarbon chain can only occur as part of certain sequences, including kinks, so that the hydrocarbon chains remain oriented within 30° of the bilayer normal, and chain packing is not disturbed. Toward the termini of the chains motion is less restricted and the population of *gauche* dihedrals and the rate of dihedral isomerization should increase.

The mean frequency of *gauche* bonds per myristoyl chain of DMPC calculated from the MD simulation is 2.6 for the Sn1 chains and 2.5 for the Sn2 chains, or 5.1 *gauche* dihedrals per DMPC molecule. From the conformational probabilities of Cevc and Marsh (1987) derived from the configurational partition function, the number of *gauche* conformations is estimated as 5.6/lipid at 55°C for a bilayer of DMPC. The data of Mendelsohn et al. (1989) on DPPC corresponds to an average *gauche* population of about six per lipid. DPPC has palmitoyl chains, which are two methylene segments longer than myristoyl. Assuming that *gauche* probability is independent of chain position this data on palmitoyl chains extrapolates to ~2.6 *gauche* conformations per myristoyl chain.

The mean frequency of kinks is calculated as 0.4/myristoyl chain from the MD simulation. Assuming that kink probability is independent of chain length, the results of Schindler and Seelig (1987) on DPPC may be extrapolated to give a frequency of 0.5 kinks/myristoyl chain. Cevc and Marsh (1987) calculate the frequency of a kink in a myristoyl chain at 55°C as 0.5.

The average chain behavior is reproduced well by the model with the simulation results nearly identical to those found from experiment and other theoretical models.

The order parameter, S_{CD}, is a measure of the motional disorder of the methylene groups in a hydrocarbon chain (Seelig and Seelig, 1974; Davis, 1983). It is calculated from Eq. 1, in which θ is the angle that the C—D bond makes with the bilayer normal. S_{CD} is obtained experimentally by measuring the quadripolar splitting of deuterium NMR signals.

$$S_{CD} = \tfrac{1}{2}(3\langle\cos^2\theta\rangle - 1). \quad (1)$$

As Petersen and Chan (1977) discuss, the value of order parameters is dependent on the method used to determine them. Electron spin resonance (ESR) experiments suggest a continuous flexibility gradient along the hydrocarbon chain, while NMR experiments exhibit a plateau. Although the ESR experiments do include the use of a probe that may perturb the system, the NMR experiments occur on a much longer time scale, and the two techniques may sample motions differently. The NMR order parameter, S_{CD}, includes both intramolecular motion and chain reorientation. If the molecule reorients about an average director, then NMR will sense the symmetry axis of this average chain orientation rather than the instantaneous chain orientation. They further suggest that chain tilt was due to individual chains tilting with respect to the bilayer normal because of motions in glycerol and ester segments, and that this tilting will be locally cooperative covering all angles within a certain range and at a rate slow compared with that for chain isomerizations. NMR cannot distinguish between a normal distribution of chains about the director and a normal distribution about a permanently tilted orientation if the chains rotate about the director. From a comparison of ^2H and ^1H order parameters, Petersen and Chan (1977) conclude that although the average tilt of the chain is parallel with the bilayer normal, the most probable tilt angle is in the range 27–34°, and the maximum tilt is ~50°. ESR experiments (Gaffney and McConnell, 1974; Birrell and Griffith, 1976) also conclude that the most probable tilt angle is nonzero and ~30°. Oldfield et al. (1978) used specifically deuterium-labeled cholesterol molecules as probes to determine molecular tilt. Although the tilt of cholesterol may not be identical to that of the lipid molecules, by extrapolating back to 0 cholesterol concentration they concluded that at 60°C the most probable tilt angle of the lipid was ~25° with respect to the bilayer normal. Using a molecular frame-and-order matrix approach Strenk et al. (1991) determined that the most ordered axis of the DMPC molecule was tilted at an angle of 27 ± 2° with respect to the bilayer normal. For the time-averaged quadripolar interaction to be parallel to the bilayer normal requires that this most ordered axis samples most orientations about the bilayer normal within the time scale of the NMR experiment, which implies either that the lipid molecule sweeps out a cone in one fixed location, or that there is rapid lateral diffusion with the molecule sampling a different orientation at each position in its lateral movement.

The experimental order parameters (Seelig and Seelig, 1974); Oldfield et al., 1978; and Rice and Oldfield, 1979) are shown in Fig. 6. Contributions to order parameter profile will include intra- and intermolecular motions, e.g., rotational isomerism between *trans* and *gauche* conformations, the rate of *gauche-trans* isomerization, and the reorientation of the lipid molecule as a whole (Mayer et al., 1988). The order parameter profiles calculated from the MD simulation shown in Fig. 7 are an average over the final 200 ps and use the SD as the source of error bars. The shape of their profile behaves in a manner similar to the NMR values. Given the caveats above concerning NMR and order parameters, the close similarity in absolute magnitude between experimental and calculated order parameters may be fortuitous. The turn in the Sn2 chain at C_{22} is retained during MD leading to the different behavior of this methylene compared with the Sn1 chain, i.e., the deuterons have different orientations (Seelig and Browning, 1978). The plateau in the order parameter profiles for the upper part of the chain near the glycerol moiety arises because the motion of the methylenes is restricted. The decrease and larger SD in the order parameter profile at the termini of the chains is due to the greater torsional and motional freedom of these methylenes. The observed difference in the magnitude of the order parameters of the Sn1 and Sn2 chains arises presumably from incomplete sampling of phase space.

After the method of van der Ploeg and Berendson (1982, 1983), the tilt of a hydrocarbon chain was calculated from the angle that a unit vector, $\mathbf{S}_i$, connecting two methylene segments of an individual hydrocarbon chain makes with the bilayer normal. The average tilt vector, $\mathbf{T}$, is the average of

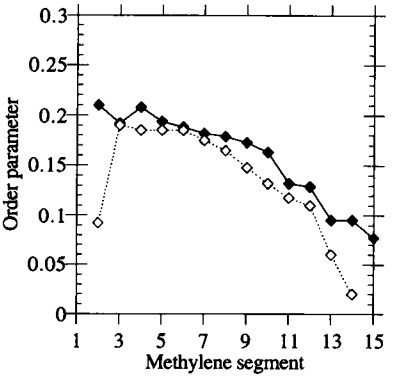

FIGURE 6 Experimental order parameter profiles from NMR quadripolar splittings for Sn1 (solid line) of DPPC (C_{32} to C_{315}; Seelig and Seelig, 1974) and Sn2 (dashed line) of DMPC (C_{22} to C_{214}; Oldfield et al. (1978), Rice and Oldfield (1979)).

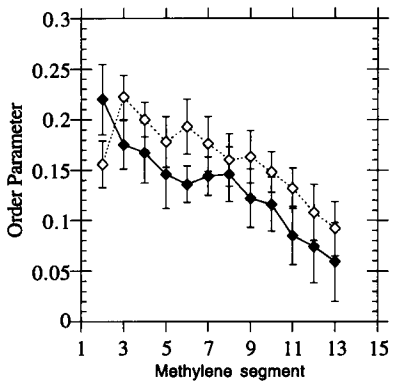

FIGURE 7 The calculated order parameter profile for the myristoyl chains from 200 ps of molecular dynamics from C_{x2} to C_{x13}. Solid line, Sn1 (x = 3); dashed line, Sn2 (x = 2). Error bars are the SD.

the N individual $\mathbf{S}_i$ vectors (Eq. 2).

$$\mathbf{T} = \frac{1}{N}\sum_{i=1}^{N}\mathbf{S}_i. \tag{2}$$

Two tilt angles were defined. The average collective tilt angle, θ_T, is the angle that **T** makes with the bilayer normal. The average individual chain tilt angle, θ_S, is the average of the angles that the individual tilt vectors $\mathbf{S}_i$ make with the bilayer normal. Fig. 8 is a normalized plot of the distribution of the tilt angles of individual chain tilt vectors for the upper and lower parts of the hydrocarbon chains. The average tilt angle of the upper vectors with respect to the bilayer normal of an Sn1 and Sn2 chain is 35.4° ∓ 14.4° SD, while the most probable tilt angle is 28.8°. The vectors of the lower part of the chain show a larger average tilt of 44.9° ∓ 19.5° SD and a most probable tilt angle of 36.3°. A portion of the chains have a tilt of greater than 90.0°. This corresponds to the chain tilt vector pointing up toward the glycerol region. For the upper part of the chain the proportion is <1%, but for the lower part of the chain the proportion is 7%, i.e., the lower part of the hydrocarbon chain has a much greater degree of freedom of motion than the upper part.

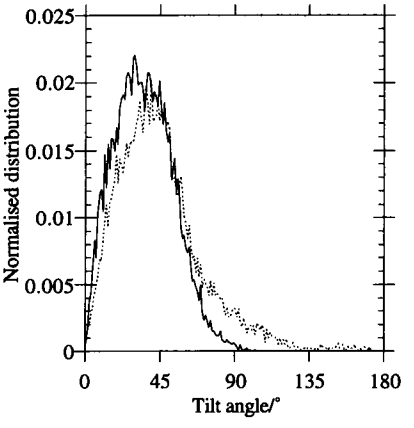

FIGURE 8 Normalized distribution of the individual chain tilt angles derived from $\mathbf{S}_i$. Solid line, upper part of the chain; dashed line, lower part.

The average collective tilt, **T**, in the upper part of the chains of one layer is 15.0° ∓ 1.9° SD, and in the other layer it is 13.7° ∓ 4.0° SD. For the lower part of the chain it is 20.1° ∓ 4.5° SD for one layer, and for the other layer it is 11.8° ∓ 4.3° SD. There is some cooperativity between the lipids leading to a collective tilt, but this is less than the individual chain-tilt angle.

It must be determined whether the system size is large enough that the collective tilt does not lead to periodic boundary violations and simulation artifacts. The properties of a system over a series of consecutive dynamics frames can be highly correlated (Allen and Tildesley, 1987). The correlation between the tilt of hydrocarbon chains was calculated from the length of **T**. As the correlation increases, the length of **T** will tend toward 1. For the upper part of the chain $|\mathbf{T}|$ is 0.78 for one layer and 0.82 for the other layer, ∓0.02 SD for both. For the lower part of the hydrocarbon chain $|\mathbf{T}|$ is 0.67 for one layer and 0.70 for the other layer, ∓0.03 SD for both. The correlation is higher near the head group where motion of the chains is restricted.

The autocorrelation function, $C(\tau)$, of S_i is defined in Eq. 3, and the time over which correlations persist for the individual chain vectors is found by fitting a simple exponential function to a plot of $C(\tau)$ versus time.

$$C(\tau) = \langle \mathbf{S}_i(t+\tau)\boldsymbol{\sigma}_i(t)\rangle. \tag{3}$$

The correlation times are 1900 ps for the upper part of the chain and 1100 ps for the lower part. The components of the autocorrelation function in the x and y directions have correlation times of about 500 ps for both the upper and lower parts of the hydrocarbon chains. These times are in excess of the simulation length and must be treated as approximate. Long autocorrelation times are not unexpected given the approximate parallel orientation of the chains that leads to large restrictions in the freedom of motion. From deuteron NMR, Mayer et al. (1988) report correlation times of 1000–100,000 ps for overall reorientation of the lipid and correlation times of 1–500 ps for intramolecular motions, i.e., correlation times of intramolecular motion occur on the same time scale as the simulations but intermolecular motions occur on a much longer time scale. The long correlation times stress the importance of a correct starting structure to avoid long equilibration times.

To measure the correlation between motions of the hydrocarbon chains a vector $\Delta r_i(t)$, which is the difference between the tilt vector, $\mathbf{S}_i(t)$, at a time t and the time average of the tilt vector for the same lipid, is defined. The correlation between two lipids, i and j, with a separation r, is a dot product calculated according to Eq. 4 over 20-ps intervals. These are averaged to provide the mean and SD for the motional correlation as a function of distance and plotted in Fig. 9.

$$C(r)dr = \left\{\frac{\langle \Delta\mathbf{r}_i(t)\cdot\Delta\mathbf{r}_j(t)\rangle}{|\Delta\mathbf{r}_i(t)||\Delta\mathbf{r}_j(t)|}\right\}dr \tag{4}$$

From the values and SDs of $C(r)$ in Fig. 9 it is apparent that the motion of the chains is correlated at separations of

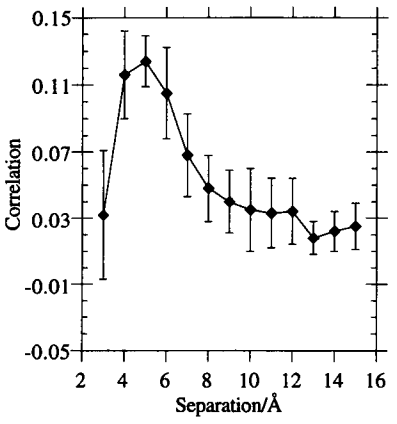

FIGURE 9 The average motional correlation of lipid chains as a function of distance using Eq. 4 over 20-ps intervals. Error bars are the SD.

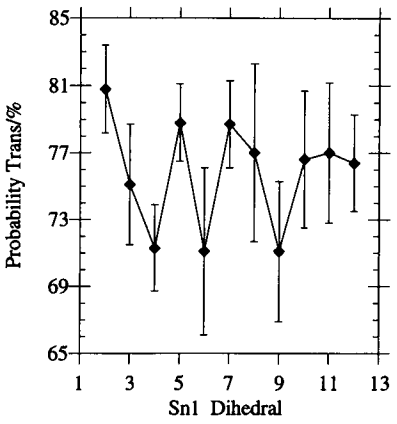

FIGURE 10 Fraction of *trans* bonds as a function of dihedral position for the Sn1 chain using the SD as the error bar values.

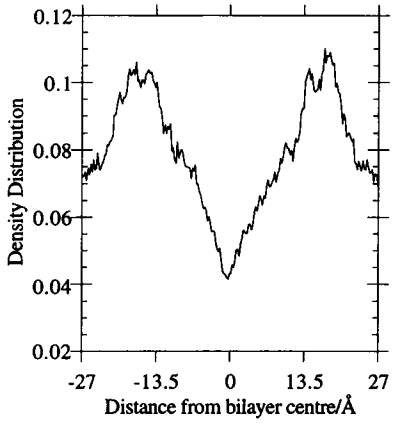

FIGURE 11 Average electron density profile across the bilayer evaluated using atom-centered electron densities over the 200 ps of molecular dynamics.

4–6 Å (corresponding to the nearest neighbors). At larger separation, the motion is on average much less cooperative, but the large SDs indicate that the motion may vary between correlated and random.

Thus the simulation reproduces the most probable tilt of a lipid chain, but the simulation is not of significant length to reach the NMR time-average tilt of 0 with respect to the bilayer normal. The collective tilt arises because the motion and tilt of a lipid chain is correlated with those surrounding it leading to local regions with a nonzero tilt of the collective chain vector. Correlations between motion do not extend beyond the nearest neighbor chains. Thus the bilayer is a mosaic of small areas, each with a nonzero collective tilt, which then averages to 0 over a larger area and time scale. We conclude that the system can successfully model individual lipids chains and their motions. Given the small number of lipids and the short simulation time compared with the time needed for chain reorientation (Mayer et al., 1988; Meier et al., 1986) it is not surprising that the 0 value of the tilt angle of the collective tilt vector cannot be reproduced.

The fraction of *gauche* bonds about a methylene segment has been estimated from NMR (Mendelsohn et al., 1989; Meier et al., 1986), although it should be emphasized that the experimental percentages are obtained by fitting NMR data to a model. The average and SD of the fraction of *trans* bonds for each dihedral along the chains is calculated from the MD simulation and presented in Fig. 10. The large values of the SD make further assumptions difficult and illustrate the long simulation times needed to reproduce accurately the properties of biological membranes.

The average electron density was evaluated over 200 ps using atom-centered electron densities for the lipid and water atoms, but to account for the head-group dipole the phosphorus was assigned 16 electrons and the nitrogen 6 (see Fig. 11). The distribution may be qualitatively compared with data from x-ray diffraction experiments on liquid crystalline DPPC at lower temperatures and relative humidities (40°C/50% r.h. and 20°C/75% r.h.) (McIntosh, 1978; Lesslauer et al., 1972). Both show the bilayer can be divided into three zones, the head groups, the apolar region, and the bilayer center. The high electron density corresponds to the closely packed head groups containing the phosphorus atoms, the fluid hydrocarbon region shows a lower density, and the dip at the center of the bilayer corresponds to the bilayer interface. The average width of the bilayer measured as the P–P distance across the bilayer is 35 ± 4 Å, which spans the experimental value of 34 ± 1 Å (Lewis and Engelman, 1983).

CONCLUSIONS

MD simulations on a model of the L_α phase of DMPC have reproduced many of the experimental observations and help further our knowledge on the dynamics and structure of biological membranes. The behavior of the fluid phase has been reproduced, the head-group layer is stable, and the presence of three conformations about the glycerol backbone has been verified. The head groups show a greater range of conformations than proposed by NMR (Seelig et al., 1977; Seelig, 1978; Skarjune and Oldfield, 1979) but are not totally conformationally flexible. The preference for *gauche* conformations in the head group may arise from the tendency of the

positive and negative parts of the lipid head group to minimize their separation. The inability to reproduce the *gauche* conformation of α_5 is probably due to a failure of the simulation technique rather than the model. The upper and lower parts of the hydrocarbon chains show different behavior with the lower part of the chain illustrating a greater freedom of motion and less correlation with neighboring chains due to the upper part of the lipid chain being motionally restricted to maintain energetically favorable chain packing. Individual chains show a nonzero tilt with respect to the bilayer normal as expected from experiments, and this leads to a local collective tilt due to cooperativity between the chains. However the simulation time is not long enough for this collective tilt to average to 0, given the long times for chain reorientation. The motion of the chains is correlated with their nearest neighbors. There are periods when correlation with more distant chains is higher, or it may fall close to 0.

The simulation of lipid bilayers is not straightforward, the starting geometry is important for successful simulations and the choice of parameter set, and long-range electrostatics play an important role. An incorrect starting geometry is unlikely to correct itself, as a change in head-group orientation will involve large concomitant changes in neighboring lipids. A head-group orientation based on that of the crystal structure appears appropriate with the lipid conformation based on results of experiments on the L_α phase. The present study represents a comprehensive starting model where the inevitable assumptions are supported by wide agreement with experiment.

AJR is supported by an SERC-CASE studentship with Glaxo Research and Development Limited. AJR would like to thank Adrian Elcock for his invaluable assistance and comments.

REFERENCES

Akutsu, H. 1981. Direct determination by Raman scattering of the conformation of the choline group in phospholipid bilayers. *Biochemistry.* 20: 7359–7366.

Akutsu, H., and T. Nagamori. 1991. Conformational analysis of the polar head group in phosphatidylcholine bilayers. A structural change induced by cations. *Biochemistry.* 30:4510–4516.

Allen, M. P., and D. J. Tildesley. 1987. Computer simulation of liquids. Oxford University Press, U.K. 385 pp.

Alper, H. E., D. Bassolino-Klimas, and T. Stouch. 1993a. Computer simulation of a phospholipid monolayer-water system: the influence of long range forces on water structure and dynamics. *J. Chem. Phys.* 98: 9798–9807.

Alper, H. E., D. Bassolino-Klimas, and T. Stouch. 1993b. The limiting behaviour of water hydrating a phospholipid monolayer: a computer simulation study. *J. Chem. Phys.* 99:5547–5559.

Bassolino-Klimas, D., H. E. Alper, and T. R. Stouch. 1993. Solute diffusion in lipid bilayer membranes: An atomic level study by molecular dynamics simulations. *Biochemistry.* 32:12624–12637.

Berendsen, H. J. C., J. P. M. Postma, W. F. van Gunsteren, A. DiNola, and J. R. Haak. 1984. Molecular dynamics with coupling to an external bath. *J. Chem. Phys.* 81:3684–3690.

Berkowitz, M. L., and K. Raghavan. 1991. Computer simulation of a water/membrane interface. *Langmuir.* 7:1042–1044.

Bicknell-Brown, E., Brown, K. G., and W. B. Person. 1982. Conformation-dependent Raman bands of phospholipid surfaces. *J. Raman Spec.* 12: 180–189.

Biswas, A., and B. L. Shurmann. 1991. Molecular dynamics simulation of a dense model bilayer of chain molecules with fixed head groups. *J. Chem. Phys.* 95:5377–5386.

Bloom, M., E. Evans, and O. G. Mouritsen. 1991. Physical properties of the fluid lipid-bilayer component of cell membranes: a perspective. *Q. Rev. Biophys.* 24:293–397.

Büldt, G., H. U. Gally, A. Seelig, and J. Seelig. 1978. Neutron diffraction studies on selectively deuterated phospholipid bilayers. *Nature.* 271: 182–184.

Büldt, G., H. U. Gally, A. Seelig, and J. Seelig. 1979. Neutron diffraction studies on phosphatidylcholine model membranes. *J. Mol. Biol.* 134: 673–691.

Büldt, G., and R. Wohlgemuth. 1981. The head group conformation of phospholipids in membranes. *J. Membr. Biol.* 58:81–100.

Cevc, G., and D. Marsh. 1987. Phospholipid bilayers. Physical properties and models. John Wiley and Sons, Inc. New York.

Charifson, P. S., R. G. Hiskey, and L. G. Pederson. 1990. Construction and molecular modelling of phospholipid surfaces. *J. Comput. Chem.* 11: 1181–1186.

Damodaran, K. V., M. Kenneth, J. Merz, and B. P. Gaber. 1992. Structure and dynamics of a dipalmitoyl phosphatidylethanolamine bilayer. *Biochemistry.* 31:7656–7664.

Damodaran, K. V., and K. M. Merz. 1993. Head group-water interactions in lipid bilayers: a comparison between DMPC- and DLPE-based lipid bilayers. *Langmuir.* 9:1179–1183.

Damodaran, K. V., and K. M. Merz. 1994. A comparison of DMPC- and DLPE-based lipid bilayers. *Biophys. J.* 66:1076–1087.

Davis, J. H. 1983. The description of membrane lipid conformation, order and dynamics by ^{2}H nmr. *Biochim. Biophys. Acta.* 737:117–171.

Dufourc, E. J., C. Mayer, J. Stohrer, G. Althoff, and G. Kothe. 1992. Dynamics of phosphate head groups in biomembranes. Comprehensive analysis using phosphorus-31 nuclear magnetic resonance lineshape and relaxation times measurements. *Biophys. J.* 61:42–57.

Edholm, O., H. J. C. Berendsen, and P. van der Ploeg. 1983. Conformational entropy of a bilayer membrane derived from a molecular dynamics simulation. *Mol. Phys.* 48:379–388.

Edholm, O., and J. Johansson. 1987. Lipid bilayer polypeptide interactions studied by molecular dynamics simulations. *Eur. Biophys. J.* 14:203–209.

Edholm, O., and A. M. Nyberg. 1992. Cholesterol in model membranes: a molecular dynamics simulation. *Biophys. J.* 63:1081–1089.

Egberts, E., and H. J. C. Berendsen. 1988. Molecular dynamics simulation of a smetic crystal with atomic detail. *J. Chem. Phys.* 89:3718–3732.

Essex, J. W. 1992. Free-energy calculations in molecular biology. Ph.D. thesis. Oxford University, U. K.

Frischleder, H., R. Krahl, and E. Lehmann. 1981. Intra- and intermolecular interactions of phospholipid head groups within a two-dimensional lattice. *Chem. Phys. Lipids.* 28:291–304.

Fukada, T., S. Okazaki, and I. Okada. 1993. Molecular dynamics study of the lauryl alcohol-laurate model bilayer. *Biophys. J.* 64:1344–1353.

Gally, H., W. Niederberger, and J. Seelig. 1975. Conformation and motion of the choline head group in bilayers of dipalmitoyl-3-*sn*-phosphatidylcholine. *Biochemistry.* 14:3647–3652

Hauser, H., I. Pascher, R. H. Pearson, and S. Sundell. 1981. Preferred conformation and molecular packing of phosphatidylethanolamine and phosphatidylcholine. *Biochim. Biophys. Acta.* 650:21–51.

Hauser, H., I. Pascher, and S. Sundell. 1988. Preferred conformation and dynamics of the glycerol backbone in phospholipids. An nmr and x-ray single-crystal structure analysis. *Biochemistry.* 27:9166–9174.

Heller, H., M. Schaefer, and K. Shulten. 1993. Molecular dynamics simulation of a bilayer of 200 lipids in the gel and in the liquid crystalline phase. *J. Phys. Chem.* 97:8343–8360.

Jorgensen W. L., J. Chandrasekhar, J. Madura, R. W. Impey, and M. L. Klein. 1983. Comparison of simple potential functions for simulating liquid water. *J. Chem. Phys.* 79:926–935.

Jorgensen, W. L., and J. Tirado-Rives. 1988. The OPLS potential functions for proteins. Energy minimizations for crystals of cyclic peptides and Crambin. *J. Am. Chem. Soc.* 110:1657–1666.

Khalatur, P. G., and A. S. Pavlov. 1987. Molecular motions in a liquid-crystalline lipid bilayer. Molecular dynamics simulation. *Makromol. Chem.* 188:3029–3040.

Lesslauer, W, J. E. Cain, and J. K. Blaise. 1972. X-ray diffraction studies of lecithin biomolecular leaflets with incorporated fluorescent probes. *Proc. Natl. Acad. Sci. USA*. 69:1499–1503.

Lewis, B. A., and D. M. Engelman. 1983. Lipid bilayer thickness varies linearly with acyl chain length in fluid phosphatidylcholine vesicles. *J. Mol. Biol.* 166:211–217.

Makino, K., T. Yamada, M. Kimura, T. Oka, and H. Ohshima. 1991. Temperature-, and ionic strength-induced conformational changes in the lipid head group region as suggested by zeta potential data. *Biophys. Chem.* 41:175–183.

Marrink, S., M. Berkowitz, and H. J. C. Berendsen. 1993. Molecular dynamics simulations of a membrane/water interface: the ordering of water and its relation to the hydration force. *Langmuir*. 9:3122–3131.

Mayer, C., G. Grobner, K. Muller, K. Weisz, and G. Kothe. 1990. Orientation dependent deuteron spin-lattice relaxation times in bilayer membranes: characterisation of the overall lipid motion. *Chem. Phys. Lett.* 165:155–161.

Mayer, C., K. Muller, K. Weisz, and G. Kothe. 1988. Deuteron N.M.R. relaxation studies of phospholipid membranes. *Liq. Cryst.* 3:797–806.

Meier, P., E. Ohmes, and G. Kothe. 1986a. Multipulse dynamic nuclear magnetic resonance of phospholipid membranes. *J. Chem. Phys.* 85: 3598–3614 .

Meier, P., E. Ohmes, G. Kothe, A. Blume, J. Weldner, and H-J. Elbl. 1986b. Molecular order and dynamics of phospholipid membranes. A deuteron magnetic resonance study employing a comprehensive lineshape model. *J. Chem. Phys.* 87:4904–4912.

Mendelsohn, R., M. A. Davies, J. W. Brauner, H. F. Schuster, and R. A. Dluhy. 1989. Qualitative determination of conformational disorder in the acyl chains of phospholipid bilayers by infrared spectroscopy. *Biochemistry*. 28:8934–8939.

McIntosh, T. J. 1978. The effect of cholesterol on the structure of phosphatidylcholine bilayers. *Biochim. Biophys. Acta*. 51:43–58.

Nagle, J. F. 1993. Area/Lipid of bilayers from NMR. *Biophys. J.* 64: 1476–1481.

Nicklas, K., J. Bocker, M. Schlenkrich, J. Brickmann, and P. Bopp. 1991. Molecular dynamics studies of the interface between a model membrane and an aqueous solution. *Biophys. J.* 60:261–272.

Oldfield, E., M. Meadows, D. Rice, and R. Jacobs. 1978. Spectroscopic studies of specifically deuterium labelled membrane systems. Nuclear magnetic resonance investigation of the effects of cholesterol in model systems. *Biochemistry*. 17:2727–2740.

Pascher, I., M. Lundmark, P. Nyholm, and S. Sundell. 1992. Crystal structures of membrane lipids. *Biochim. Biophys. Acta*. 1113:339–373.

Pascher, I., and S. Sundell. 1986. Membrane lipids: preferred conformational states and their interplay. The crystal structure of dilauroylphosphatidyl-*N,N*-dimethylethanolamine. *Biochim. Biophys. Acta*. 855: 68–78.

Pearson, R. H., and I. Pascher. 1979. The molecular structure of lecithin dihydrate. *Nature*. 281:499–501.

Petersen, N. O., and S. I. Chan. 1977. More on the motional state of lipid bilayer membranes: interpretation of order parameters obtained from nuclear magnetic resonance experiments. *Biochemistry*. 16: 2657–2667.

Rice, D., and E. Oldfield. 1979. Deuterium nuclear magnetic resonance studies of the interaction between dimyristoylphosphatidylcholine and Gramicidin A. *Biochemistry*. 18:3273–3279.

Ryckaert, J. P., G. Ciccotti, and H. J. C. Berendsen. 1977. Numerical integration of the cartesian equations of motion of a system with constraints: molecular dynamics of *n*-alkanes. *J. Comput. Phys.* 23:327–341.

Schindler, H., and J. Seelig. 1987. Deuterium order parameters in relation to thermodynamic properties of a phospholipid bilayer. A statistical mechanical interpretation. *Biochemistry*. 14:2283–2287.

Seelig, J. 1978. ^{31}P nmr and the head group structure of phospholipids in membranes. *Biochim. Biophys. Acta*. 515:105–140.

Seelig, J., and J. L. Browning. 1978. General features of phospholipid conformation in membranes. *FEBS Lett.* 92:41–44.

Seelig, J., H. Gally, and R. Wohlgemuth. 1977. Orientation and flexibility of the choline head group in phosphatidylcholine bilayers. *Biochim. Biophys. Acta*. 467:109–119.

Seelig, J., and A. Seelig. 1974. The dynamic structure of fatty acyl chains in a phospholipid bilayer measured by deuterium magnetic resonance. *Biochemistry*. 13:4839–4845.

Singh, U. C., P. K. Weiner, J. W. Caldwell, and P. A. Kollman. 1988. AMBER (Version 3.1). Department of Pharmaceutical Chemistry, University of California, San Francisco.

Skarjune, R., and E. Oldfield. 1979. Physical studies of cell surface and cell membrane structure. Determination of head group organisation by deuterium and phosphorus nmr spectroscopy. *Biochemistry*. 18:5903–5909.

Stouch, T. R. 1993. Lipid membrane structure and dynamics studied by all-atom molecular dynamics simulations of hydrated phospholipid bilayers. *Mol. Sim.* 10:317–345.

Stouch, T. R., H. E. Alper, and D. Bassolino. 1994. Supercomputing studies of biomembranes. *Int. J. Supercomput. Applications*. In press.

Stouch, T. R., K. B. Ward, A. Altieri, and A. T. Hagler. 1991. Simulations of lipid crystals: characterisation of potential energy functions and parameters for lecithin molecules. *J. Comp. Chem.* 12:1033–1046.

Strenk, L. M., P. W. Westerman, and J. W. Doanne. 1991. A model of orientational ordering in phosphatidylcholine bilayers based on the conformational analysis of the glycerol backbone region. *Biophys. J.* 48: 765–773.

Sundaralingham, M. 1972. Molecular structures and conformations of the phospholipids and sphingomyelins. *Ann. N. Y. Acad. Sci.* 195:324–355.

van der Ploeg, P. and H. J. C. Berendsen. 1982. Molecular dynamics simulation of a bilayer membrane. *J. Chem. Phys.* 76:3271–3276.

van der Ploeg, P. and H. J. C. Berendsen. 1983. Molecular dynamics of a bilayer membrane. *Mol. Phys.* 49:223–248.

Venable, R. M., Y. Zhang, B. J. Hardy, and R. W. Pastor. 1993. Molecular dynamics simulations of a lipid bilayer and hexadecane. An investigation of membrane fluidity. *Science*. 262:223–226.

Xiang, T. 1993. A computer simulation of free-volume distributions and related structural properties in a model lipid bilayer. *Biophys. J.* 65:1108–1120.

Yeagle, P. 1977. Phospholipid headgroup conformation. Intermolecular interactions and cholesterol effects. *Biochemistry*. 16:4344.